



Magnetic turbulence in the shock precursor and cosmic ray acceleration

A. Beresnyak

Ruhr-Universität Bochum – 44780 Bochum, Germany, e-mail: ab@tp4.rub.de

Abstract. We overview recent progress on small-scale dynamo and apply the results to the problem of nonlinear shock acceleration in which particle mean free paths in front of the shock are greatly reduced due to magnetic fields in the shock precursor which are generated through small-scale dynamo in the density gradient's-induced turbulence. Previous DSA models considered magnetic fields amplified through cosmic ray streaming instabilities either by way of individual particles scattering in the magnetic fields, or by macroscopic electric currents associated with large-scale cosmic ray streaming. The small-scale dynamo mechanism provides fast growth and is very generic. For supernovae shocks this mechanism is estimated to generate upstream magnetic fields that are sufficient for accelerating cosmic rays up to around 10^{16} eV.

Key words. MHD – turbulence – cosmic rays: acceleration

1. Introduction

Diffuse γ -ray emission from the Galaxy, detected by EGRET, Fermi and other missions has been explained by interaction of galactic cosmic rays (CRs) with interstellar medium, molecular clouds and interstellar magnetic fields. Pion production by protons and nuclei and inverse Compton (IC), bremsstrahlung and synchrotron emission by electrons and positrons all contribute to observed γ -ray emission. Cosmic rays, relativistic charged particles with energies $10^8 - 10^{22}$ eV, constitute an essential part of astrophysical systems (see Schlickeiser 2003). In galaxies they provide pressure and energy densities comparable to those of magnetic fields and thermal gas. In very dense regions, such as the cores of molecular clouds or accretion disks they are the only source of ionization that that must be present to allow interaction of magnetic field and the

fluid. The origin of CRs has been a subject of debate from the beginning of research in the field (Ginzburg & Syrovatsky 1964). It could be argued from energetic constraints that galactic CRs at least up to the “knee” in the spectrum (10^{15} eV) are most likely generated by supernova shocks.

However, the upstream magnetic fields of the ISM, $5\mu\text{G}$, are too weak to provide an efficient acceleration of the cosmic rays with energies as high as 10^{15} GeV. Such PeV cosmic rays will have long mean free paths and have a high probability of escaping, after which they are not subject to further acceleration. This poses a serious problem for the shock acceleration of galactic CRs.

To overcome the problem one can argue that the magnetic field in the preshock region can be much stronger than its interstellar value and that the free energy avail-

able for the shock is sufficient to generate much larger fields (Volk, Drury & McKenzie, 1984). The magnetic field generation, if pursued through streaming instability, leads naturally to a highly nonlinear stage of the streaming instability where $\delta B \gg B_0$. The original classical treatment of the instability is not applicable in that limit. What happens in the non-linear regime has been a subject of much discussion in recent years (e.g., Lucek & Bell 2000, Diamond & Malkov 2007, Blasi & Amato 2008, Riquelme & Spitkovsky 2009). The current driven instability proposed by Bell (2004) has moved recently to the center of this debate. The driving electric current of the instability comes from drift (streaming) of the escaping CRs. The *compensating* return current of the background plasma leads to a transverse force on the background plasma that can amplify transverse perturbations in the magnetic field. Numerical simulations suggest that the initial field strength can grow substantially, leading in the nonlinear form to disordered fields with coherence lengths that depend on field strength. In what follows, we argue that there is a process that can provide fast magnetic field generation. It provides sufficiently strong magnetic field without appealing to either classical streaming instabilities or their modifications. The CR pressure gradient is the dynamical agent that forms the shock precursor and also drives field amplification.

We assume that the CR pressure is a smooth function applied to the fluid, while the magnetic field is generated by purely fluid nonlinear mechanisms. The magnetic field, in turn, scatter CRs. The fluid is stirred within the precursor on large, precursor-sized, scales by the combination of ISM density inhomogeneities and CR pressure. In particular, the vorticity is generated directly by $\nabla \rho_{ISM} \times \nabla P_{CR}$ baroclinic term, as CR pressure is not barotropic with respect to the ISM density (and not even a function of this density). Although we consider the CR pressure applied to the inflowing fluid homogeneous in the direction along the shock, the acceleration of the fluid element is highly inhomogeneous due to the density inhomogeneity of the fluid. This drives precursor

turbulence. Magnetic energy is generated on intermediate scales by a small-scale dynamo.

2. Small-scale dynamo

In this paper we only consider turbulence hydrodynamically amplified within the precursor. We do not consider post-shock turbulence, which is a fairly well-known and better explored phenomenon that exists even in pure hydrodynamics without a CR precursor (see, e.g., Giacalone & Jokipii, 2007).

As inhomogeneous fluid flows into the precursor with speed u_0 it is gradually decelerated by the CR pressure gradient until it reaches the speed u_1 at the dissipative shock front. This deceleration could create vortical perturbations of velocity of the order $u_0 - u_1$, a difference between ballistic velocity of the high-density region and full deceleration of the low density regions. It is due to the baroclinic term $\nabla \rho_{ISM} \times \nabla P_{CR}$ that breaks Kelvin circulation theorem in every sub-volume of the fluid. Cosmic ray pressure P_{CR} provides an external (non-fluid) force ∇P_{CR} which is not barotropic with respect to the plasma density ρ_{ISM} .

Three-dimensional solenoidal flows can amplify magnetic fields through the stretch-fold mechanism. We will consider a so-called generic small-scale dynamo (turbulent) in which magnetic fields are amplified by initially weakly magnetized hydrodynamic turbulence with an energy-containing (outer) scale of L . “Small-scale” means that the scales of magnetic fields we are interested in are smaller than L . The problem of the so-called mean-field dynamo, when *large-scale* magnetic fields are generated by small-scale motions is not considered here, because the mean-field dynamo is fairly slow (see Vishniac & Cho 2001), while inside the shock precursor the time for the amplification is rather limited, since all perturbations are quickly advected to the dissipative shock. The small-scale dynamo has three principal stages – a kinematic stage, when magnetic energy grows exponentially, a linear stage and a saturation stage (see Cho et al, 2009).

For astrophysical applications the kinematic dynamo is irrelevant, since its characteristic saturation timescale is of the order of

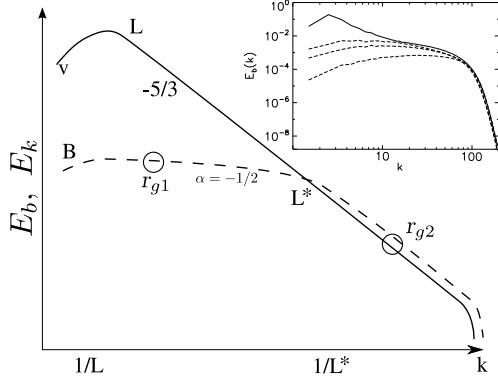


Fig. 1. Magnetic spectrum (dashed), generated by small-scale dynamo induced by solenoidal velocity motions (solid). L^* is an equipartition scale of magnetic and kinetic motions. Upper panel: magnetic and velocity fields from simulations (Cho et al 2009). Dashed lines are magnetic spectra at different times.

an eddy turnover time of the smallest eddies, which is a tiny number compared to outer timescales. For our purposes we can always assume that the kinematic dynamo is saturated and the dynamo is in the linear stage.

In the linear stage magnetic energy grows linearly with time as

$$\frac{1}{8\pi} \frac{dB^2}{dt} = A_d \epsilon, \quad (1)$$

where ϵ is the energy transfer rate of the turbulence, which can be estimated as $\epsilon = \rho u_s^3/L$, and A_d can be called an *efficiency of the small-scale dynamo*. A typical spectrum of the velocity and the magnetic field in the linear stage is presented on Fig. 1. At each particular time the magnetic field reaches equipartition with the turbulent velocity field on some scale L^* . This scale grows with time. On scales smaller than L^* magnetic and velocity perturbations form an MHD turbulent cascade with a fairly steep spectrum. On scales larger than L^* , the magnetic field has a fairly shallow spectrum and velocity has a Kolmogorov spectrum.

The law of linear growth can be understood as follows. The main cascade of energy is down-scale, but it is converted from a purely

velocity cascade to an MHD cascade at a scale L^* . One can imagine that part of this energy cascades up (an inverse cascade) in the form of magnetic energy. Let us call this fraction A_d . In principle, A_d can depend on scale, i.e., $A_d(L^*)$. However, by an argument similar to Kolmogorov's, if the inverse cascade mechanism is purely nonlinear, then, in the middle of the inertial interval there is no designated scale and, therefore, there is no dimensionless combination involving L^* . Therefore, the function $A_d(L^*)$ has to be constant. This gives a linear growth of energy. The linear growth can also be obtained if we assume that it takes *several* turnover times to reach equipartition on each successive step to larger and larger L^* . A linear growth rate has been measured in Cho et al. (2009) as being close to $A_d \approx 0.06$ which is the quantity we will use in this paper.

The shallow part of the magnetic spectrum between L and L^* normally has a slope α between 0 and -1 , as observed in simulations. We will need these constraints later, when we describe a model of particle scattering. We particularly favor a model with $\alpha = -1/2$. This model assumes that while magnetic fields on a scale L^* are generated by random eddies at the same scale L^* and contain most of the magnetic field energy, the larger scale fields come from equipartition of magnetic tension on scale $l > L^*$. This can be estimated as $\delta B^2(l)/l$, while the averaged magnetic tension comes from a number $N = (l/L^*)^3$ of independent random eddies on scale L^* . This will give scalings $\delta B(l) \sim l^{-1/4}$ and

$$E_B(k)k = \delta B^2(k) \sim k^{1/2}. \quad (2)$$

When L^* approaches L , the small-scale dynamo enters the saturation stage in which the magnetic field grows more slowly than in the previous linear stage. The saturation value of magnetic energy depends slightly on the level of the mean magnetic field (Cho et al. 2009). In our case the *mean* magnetic field can be considered negligible, as the typical Alfvén velocity of warm ISM (~ 12 km/s) is much smaller than the shock speed and associated turbulent speeds. For the purpose of this paper, however, we won't need a saturation stage, since

we have limited time available for amplification, τ_c , which is normally not enough to reach the saturation stage.

From the linear stage growth we derive quantities $\delta B^* = \delta B(L^*, x_1)$ and $L^*(x_1)$ that we will need in the next section:

$$\delta B^2(L^*, x_1) = 8\pi A_d \epsilon \tau(x_1); \quad (3)$$

$$\frac{\delta B^*}{\sqrt{4\pi\rho}} = u_s \left(\frac{L^*(x_1)}{L} \right)^{1/3}; \quad (4)$$

$$\tau(x_1) = \int_{x_1}^{x_0} \frac{dx}{u(x)}; \quad (5)$$

$$L^*(x_1) = (2A_d u_s \tau(x_1))^{3/2} L^{-1/2}. \quad (6)$$

3. Measurements of scattering in DNS of MHD turbulence

It was argued in Yan & Lazarian (2002, 2004) that fast mode should dominate particle scattering in MHD turbulence. Fast mode, however, is often damped. In particular, strong TTD damping is expected in low-collisional environments, such as hot ISM, which is often a medium in which strong supernova shocks propagate. In this case fast mode will be effectively absent. It is, however, interesting to check the prediction of so-called Quasilinear Theory (QLT, see, e.g., Schlickeiser 2002) that scattering by incompressible components, Alfvén and slow waves is basically absent (Chandran 2000).

We traced particle trajectories in electromagnetic fields obtained in direct three-dimensional simulations of MHD turbulence. We used driven simulations described in more detail in Beresnyak & Lazarian 2009(a,b). The electric field in the laboratory frame was obtained through $E = -[v \times B]/c$, assuming typical ISM value of $v_A/c = 10^{-5}$. The particles were injected randomly through the datacube and the trajectories for the relativistic equations of motion were traced by hybrid Runge-Kutta quality-controlled ODE solver, assuming periodic boundaries for particles and fields.

$D_{\mu\mu}$ scattering property was measured in the tracing experiments where an ensemble of particles with the same r_L (energy) and a particular μ_0 were traced by a certain time. This

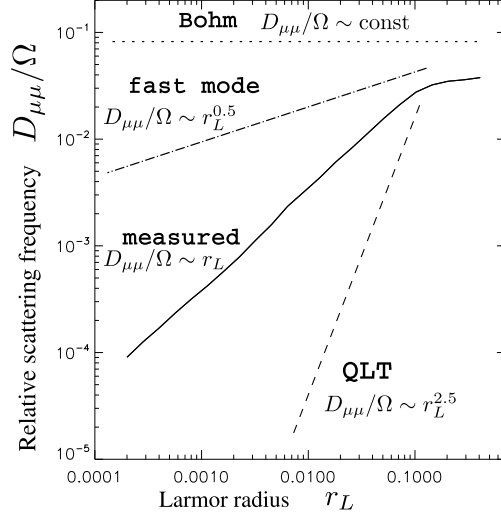


Fig. 2. Measured scattering coefficient $D_{\mu\mu}/\Omega$ ($\mu_0 = 0.71$) vs Larmor radius r_L in cube size units (solid line). For comparison, we plot various theoretical predictions: QLT prediction for Alfvén and slow mode (dashed); QLT prediction for fast mode (dot-dashed); hypothetical Bohm scattering or maximally efficient scattering (dotted).

time was determined by the condition that the RMS of deviations of μ is small (i.e. 0.1-0.01). Then the curves of the ensemble-averaged $\langle(\mu - \mu_0)^2\rangle$ were fitted with a linear curve.

As we see from Fig. 2 the measurement of scattering frequency is incompatible with QLT. The scattering frequency normalized to the gyration frequency is proportional to the Larmor radius i.e. it is constant with energy (as $\Omega r_L = v \approx c$). It would be reasonable to assume then that particles of all energies scatter on the same objects, magnetic bottles, formed by large scale slow-mode perturbations. The same result could be obtained from nonlinear scattering theory (Yan & Lazarian 2008), taking into account $\Delta\mu \sim \mu$ in strong turbulence. At larger energies scattering becomes less efficient i.e. high energy particles “feel” less mirrors. This transition happens at around $r_L/L \approx 0.1$.

4. Particle scattering and second-order acceleration

As it turns out, there are three different regimes of particle scattering, depending on the particle energy, E , (see Fig. 3). The magnetic spectrum, described in Fig. 1, corresponds to the characteristic magnetic field on a particular scale $\delta B(l) \sim \sqrt{E(k)k}$, which increases with decreasing scale as $l^{-\alpha/2-1/2} = l^{-1/4}$ for $\alpha = -1/2$ from L until L^* and decreases with scale as $l^{1/3}$ for l smaller than L^* .

If the particle energy is sufficiently low, the particle will, to the first approximation, gyrate around a mean field. Otherwise, its trajectory will be stochastic. In particular, if $E \ll e\delta B(L^*)L^*$, the particle will be gyrating along the mean field of $\delta B^* = \delta B(L^*)$ with Larmor radius of $r_{g2} = E/e\delta B^*$. We will refer to these particles as low-energy and designate low energies as region (1) in Fig. 3. For low energy particles the scattering frequencies and acceleration will be determined by a turbulence-based formulae with turbulence outer scale of L^* (the scale with largest magnetic field). We will consider this case in detail in the next section.

4.1. High energy particle scattering

If the energy of the particle is higher than $e\delta B(L^*)L^*$, there is no gyration and the particle's trajectory is fairly stochastic. This is due to the fact that for this particle, the vector magnetic field will be partially averaged out on larger scales (so that $\delta B_l \sim l^{-1/4}$). Let us assume that such a particle experience a Bohm scattering and have a *mean free path* of

$$\begin{aligned} r_{g1} &= (E/e\delta B^*)^{\frac{2}{1-\alpha}} (L^*)^{-\frac{1+\alpha}{1-\alpha}} \\ &= (E/e\delta B^*)^{4/3} (L^*)^{-1/3} > L^*. \end{aligned} \quad (7)$$

Indeed, (a) – on such a scale, a particle will be deflected by an angle of the order of unity; (b) – the deflection from larger scale field will be smaller (if $l_2 > r_{g1}$, then the deflection angle $e\delta B(l_2)r_{g1}/E < 1$); (c) – the deflection from some smaller scale l_1 is also smaller (it is a random walk with r_{g1}/l_1 steps), and the deflection angle is $e\delta B(l_1)l_1^{1/2}r_{g1}^{1/2}/E < 1$. Assuming

$E = pc$ from here on, the D_{xx} and D_{pp} for such particles will be determined by velocity perturbations on scale r_{g1} , i.e., $u_s r_{g1}^{1/3} L^{-1/3}$; thus,

$$D_{xx} = (E/e\delta B^*)^{4/3} (L^*)^{-1/3} c, \quad (8)$$

$$D_{pp} = p^2 u_s^2 r_{g1}^{-1/3} L^{-2/3} / c \propto E^{14/9} \quad (9)$$

Finally, for very high energy particles

$$E \gg e\delta B^* L^{\frac{1-\alpha}{2}} (L^*)^{\frac{1+\alpha}{2}} = e\delta B^* L^{3/4} (L^*)^{1/4}, \quad (10)$$

the trajectory will be a random walk with small deflections from scale L and an effective mean free path of $E^2/e^2\delta B_L^2 L$. The D_{pp} will be energy independent, as it will be set by outer scale velocity perturbations of u_s . So,

$$D_{xx} = E^2 c / e^2 \delta B_L^2 L, \quad (11)$$

$$D_{pp} = (e\delta B_L)^2 L u_s^2 / c^3. \quad (12)$$

4.2. Low energy particle scattering

For the purpose of this paper we will consider two simple, contrasting cases. In the first case, we will assume that the fast mode is fully damped and that only solenoidal modes survive on scales of L^* and smaller. This case was considered in the previous section. We can neglect QLT contributions from the Alfvénic and slow modes as they are very small. On the other hand, there are strong perturbations of the magnetic field on the outer scale of L^* . In this case particles, regardless of energy (provided that $E \ll e\delta B(L^*)L^*$) are going to be reflected by magnetic bottles on scale L^* and D_{xx} will be independent of energy and equal to L^*c , and D_{pp} will be determined by the speed of the bottles:

$$D_{xx} = L^*c, \quad (13)$$

$$D_{pp} = p^2 u_s^2 (L^*)^{-1/3} L^{-2/3} / c. \quad (14)$$

In the second case, we will assume that the fast mode is not damped and that the scattering and second-order acceleration are due to the fast mode. If we assume that the amplitude

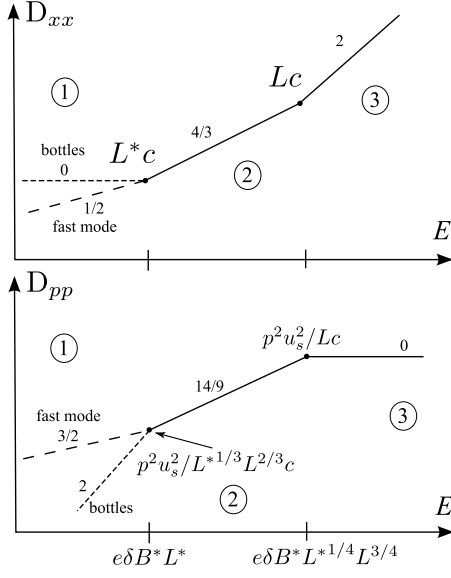


Fig. 3. Diffusion coefficients D_{xx} and D_{pp} vs energy. There are three regimes: (1), a low-energy scattering, which depends on the properties of small-scale MHD turbulence, two cases where fast modes are present (dashed) and absent (dotted) are shown; (2), the strong scattering, where particles are scattered efficiently by the large magnetic fields, generated by small-scale dynamo; (3), at high-energies particles are only slightly refracted.

of the fast mode is approximately in equipartition with other modes on the outer scale of sub-Alfvénic turbulence, L^* , we will obtain:

$$D_{xx} = cr_{g2}^{1/2}(L^*)^{1/2}, \quad (15)$$

$$D_{pp} = p^2 u_s^2 (L^*)^{1/6} L^{-2/3} r_{g2}^{-1/2}. \quad (16)$$

Here we have used so-called acoustic turbulence scaling $\delta B \sim l^{1/4}$ for the isotropic fast mode, as in Cho & Lazarian (2002). The shock precursor with its high density of CRs could be affected by collective effects where compressions of magnetic field induce the gyroresonance instability as discussed in Lazarian & Beresnyak (2006). We skip discussion on this complex subject here.

5. Acceleration

The self-consistent treatment of the flow profile and acceleration of particles using expressions from above will be presented in a future publication. The scattering coefficients assume that efficient scattering will be experienced by particles with energies up to $E_{2-3} = e\delta B^* L^{*1/4} L^{3/4}$ (see Fig. 3). This energy can be estimated taking $u_s \tau \approx L$, $u_s \approx 10^4 \text{ km/s}$ and $L \approx 1 \text{ pc}$ and $E_{2-3} \approx 3 \times 10^{17} \text{ eV}$. As this energy corresponds to a mean free path of the order of L and the acceleration efficiency is smaller by a factor of u_s/c (Hillas, 1984) the maximum acceleration energy will be around 10^{16} eV . The higher energy particles will be scattered relatively less efficiently and will form a steep cut-off spectrum.

References

- Bell, A. R. 2004, MNRAS, 353, 550
 Beresnyak, A., Lazarian, A. 2009a, ApJ, 702, 460; 2009b, ApJ, 702, 1190
 Blasi P. & Amato, E. 2008, 2008ICRC, 2, 235
 Chandran B.D.G. 2000, Phys. Rev. Lett., 85, 4656
 Cho, J. & Lazarian, A. 2002, Phys. Rev. Lett., 88, 5001
 Cho, J., Vishniac, E., Beresnyak, A., Lazarian, A., & Ryu, D. 2009, ApJ, 693, 1449
 Diamond, P.H., Malkov, M.A. 2007 ApJ, 654, 252
 Ginzburg, V. & Syrovatskii, S. 1964, Origin of Cosmic Rays, Pergamon Press, NY
 Giacalone J., Jokipii, J.R. 2007, ApJ, 663, L41
 Hillas, A. M. 1984 ARA&A, 22, 425
 Lazarian, A., Beresnyak, A. 2006, MNRAS, 373, 1195
 Riquelme, M. A. & Spitkovsky, A. 2009, ApJ, 694, 626
 Schlickeiser, R. 2002, *Cosmic Ray Astrophysics* (Springer-Verlag: Berlin)
 Vishniac, E. T., Cho, J. 2001, ApJ, 550, 752
 Völk, H.J., Drury, L.O'C., & McKenzie, J.F. 1984, A&A, 130, 19
 Yan, H. & Lazarian, A. 2002, Phys. Rev. Lett., 89, 1102
 Yan, H. & Lazarian, A., 2004, ApJ, 614, 757
 Yan, H. & Lazarian, A., 2008, ApJ, 677, 1401